PHYSICAL REVIEW A VOLUME 56, NUMBER 3 SEPTEMBER 1997

HgIn photoassociation, bound-bound transitions, and excimer emission

P. Bicchi,[1] C. Marinelli,[1] and R. A. Bernheim[2]
[1]*INFM and Department of Physics, University of Siena, Via Banchi di Sotto 55/57, 53100 Siena, Italy*
[2]*Department of Chemistry, Penn State University, 152 Davey Laboratory, University Park, Pennsylvania 16802*

(Received 21 April 1997)

Laser excitation of In atoms at the $6\,^2S_{1/2}$–$5\,^2P_{1/2}$ atomic resonance transition wavelength of 410.3 nm in the presence of Hg vapor produces several types of emission features: HgIn excimer satellites on the red wings of the In resonance fluorescence transitions at 410.3 and 451.1 nm, bound-bound HgIn molecular fluorescence at 499 and 522 nm resulting from photoassociation of In($6\,^2S_{1/2}$) with Hg($6\,^1S_0$), and UV atomic fluorescence from the In($5\,^2D$) states that lie at energies above the In($6\,^2S_{1/2}$–$5\,^2P_{1/2}$) excitation. These various spectral features are interpreted in terms of a proposed HgIn potential-energy level diagram with additional information from measured excited-state lifetimes and the power dependence of the laser excitation at 410.3 and 522 nm. Direct excitation of the 499 and 522 nm HgIn bound-bound transitions also produces emission at 410.3 and 451.1 nm resulting from collisional dissociation of the excited HgIn states. [S1050-2947(97)10109-3]

PACS number(s): 34.50.Gb, 34.20.Cf, 33.20.Kf, 42.55.Lt

I. INTRODUCTION

Over the past several decades considerable attention has been given to excimers derived from metal–noble-gas dimers. With their $^1S_0$ closed-shell electronic ground states, the noble-gas elements give rise to mainly dissociative ground-state interactions with the metal atoms [1], thereby providing the lower state for the excimer emission. As an alternative to the noble gases, group-II elements with their $^1S_0$ closed sub-shell electronic ground states often provide mainly dissociative ground states in their interaction with many metal atoms. Among the group-II elements, mercury is a particularly attractive excimer partner because of its considerable vapor pressure and its low-lying, easily excited electronic states. That it is a viable candidate as an atomic partner for an excimer laser is evidenced by the fact that stimulated emission has been observed in mercury halides [2]. Since a high rate of excitation is required for laser gain, those metal atoms with low-lying excited electronic states are also considered to be good candidates for excimer lasers as they can be expected to have large cross sections for electronic excitation. However, the dissociative nature of the Hg-metal ground states is also a factor. For example, HgTI has been advanced as an attractive group-II–group-III excimer laser possibility [1], but gain has yet to be observed for this system [3].

The element In occurs immediately above T1 in the group-III metals and has the unusual property that its $6\,^2S_{1/2}$ first excited atomic resonance state at $24\,372.87\ \mathrm{cm}^{-1}$ is greater in energy than one-half of the In $46\,669.93\text{-}\mathrm{cm}^{-1}$ ionization potential [4]. Besides offering a $1+1$ multiphoton ionization (MPI) process, this situation also forms the basis for the very interesting energy pooling ionization collisions [5,6]:

$$\mathrm{In}(6\,^2S_{1/2})+\mathrm{In}(6\,^2S_{1/2})\rightarrow\mathrm{In}^+(^1S_0)+\mathrm{In}(5\,^2P_{1/2})+e^-,$$

which may play a role in electrical discharge excitation at high metal vapor densities.

Although excimers can be created by a variety of excitation methods, their structure and dynamics are often best studied when they are formed from collisions in which one of the atoms is prepared in a single, discrete excited state. This is conveniently accomplished for the group-III metals using laser excitation of the atomic resonance transitions. The present work was undertaken to examine the emission characteristics of electronically excited HgIn generated as the photoassociation product between laser excited In($6\,^2S_{1/2}$) and ground-state Hg($6\,^1S_0$) atoms and to examine the nature of the upper and lower electronic states that correlate with this emission.

In electrical discharges, emission spectra [7–11] that have been identified as arising from HgIn consist of (a) the excimer wings and satellites associated with the 410.3- and 451.1-nm In atomic lines, and (b) electronic band spectra of HgIn at 522 and 499 nm. These spectroscopic features were first observed by Winans *et al.* [7] and later studied by Purbrick [8], Chilikuri and Winans [9], and Thomson *et al.* [10]. More recently they were observed in an electrical discharge by Pichler *et al.* [11], who discussed the excimer wings on the In atomic lines in terms of an HgIn potential energy diagram constructed by analogy with the results of HgTl *ab initio* calculations [12]. The prominent HgIn excimer emission features in electrical discharges are the red-wing satellites at 412.7 nm for the 410.3-nm In atomic line and at 453.7 nm for the 451.1-nm In atomic line [8,11]. Additional weaker satellites are also observable [11]. The resolved rovibrational structure of the bound-bound HgIn electronic band spectra at 522 nm has had several interpretations. The first of these [8] proposed a long progression ($v'=0-14$) terminating on $v''=0$ in the lower state. However, these bands were later reinterpreted by Chilukuri and Winans [9] as being due to two overlapping sequences $B\,^2\Pi_{1/2}$–$A\,^2\Sigma$ and $B\,^2\Pi_{3/2}$–$A\,^2\Sigma$. The basis for the revision was an analogy with the (B-A) bands of CdIn and ZnIn where P and Q band heads and overlapping doublet sequences were clearly evident. The atomic states that asymptotically correlate with the upper and lower electronic states of the 522-nm band have also received different assignments. Chilukuri and Winans

[9] suggested that these might be Hg(^3S)+In($5\,^2P_{1/2}$) for the upper state and Hg(^3P)+In($5\,^2P_{1/2}$) for the lower state. More recently, Thomson *et al.* observed the band at 522 nm together with a more intense broad band at 505 nm when In atoms are excited to the $6\,^2S_{1/2}$ state in an experiment where the In atoms are generated by photodissociation of InBr in the presence of mercury vapor [10]. Their conclusions were that the 522-nm band could be assigned to emission arising from a bound excimer state of HgIn correlating with the In($6\,^2S_{1/2}$)+Hg($6\,^1S_0$) asymptote, and that the 505-nm band was due to In($6\,^2S_{1/2}$) interacting with InBr.

As shown in the present study, excitation of In vapor at 410.3 nm in the presence of Hg vapor produces, in addition to the 499- and 522-nm bands, UV emission from the higher-energy In($5\,^2D$) states, which forces one to consider the possibility that the 522-nm band might originate from a state correlating with In atomic states above In($6\,^2S_{1/2}$) or from a state correlating with one of the In atomic ground states and excited states of Hg. Furthermore, the fluorescence decay time of the 522-nm band was found to have both a fast and a slow component. Other findings that must be reconciled with the assignment of the bound-bound transitions are the currently accepted spectroscopic constants for the 522-nm band [9], which are $v_e=19,106\ \mathrm{cm}^{-1}$, $\omega'_e=198\ \mathrm{cm}^{-1}$, $\omega''_e=151\ \mathrm{cm}^{-1}$ with anharmonic constants $\omega'_e x'\approx\omega''_e x''_e\approx 0$. The negligible anharmonic constants together with the ω_e values are an indication of a substantial bond energy for the upper and lower states of HgIn, which give rise to this band.

The present work offers additional spectroscopic findings that are interpreted in terms of a proposed potential energy level structure for HgIn.

II. EXPERIMENT

The measurements were carried out in a quartz sample cell 3 cm in diameter by 5 cm in length loaded with a small piece of In metal of 99.999% stated purity [13]. A very small droplet of mercury is added and the cell degassed under vacuum at 473 K. After filling with 10 torr of Ne gas, the cell is sealed off. At the temperature of 1173 K where most of the measurements were made, the mercury is entirely vaporized with an atomic number density of approximately $10^{19}\ \mathrm{cm}^{-3}$. The In atomic number density [14] is $6.5\times10^{13}\ \mathrm{cm}^{-3}$ and the Ne atomic density is $8.2\times10^{16}\ \mathrm{cm}^{-3}$. The cell is placed in an oven where a long-term temperature stability of 1 K could be maintained for the measurements.

Resonant excitation of In atoms to the $6\,^2S_{1/2}$ level is produced by pulsed laser radiation at 410.3 nm obtained by optical mixing the output of a pulsed dye laser at 667 nm with the 1064-nm fundamental of a Nd:YAG laser. The pulses at 10 Hz have a 10-ns width and a 0.8-cm^{-1} bandwidth, mainly due to that of the fundamental Nd:YAG output. Laser power densities range between 0.2 and $3.4\ \mathrm{MW/cm}^2$ in a beam diameter of approximately 3 mm.

For the direct excitation of HgIn in the 490–525-nm region, the pulsed radiation produced by the dye laser was used directly and with a bandwidth of $0.3\ \mathrm{cm}^{-1}$. The power densities quoted for those experiments are for 10-Hz, 10-ns pulse duration, and in a 3-mm-diameter beam.

The laser-induced fluorescence at 90° is dispersed with a Jobin Yvon HR1000 monochromator at 15-cm^{-1} resolution and detected with a Hamamatsu R663 photomultiplier. For the lifetime measurements the output of the photomultiplier is monitored with a Tektronix TDS520 transient digitizer having a 500-MHz bandwidth. Spectra as a function of either dispersed fluorescence or scanned excitation wavelength were recorded using a boxcar averager. The In atomic spectral lines provide a convenient wavelength calibration. The laser power was measured at both the beginning and end of each data collection experiment with an Ophir 10 A-P laser power meter.

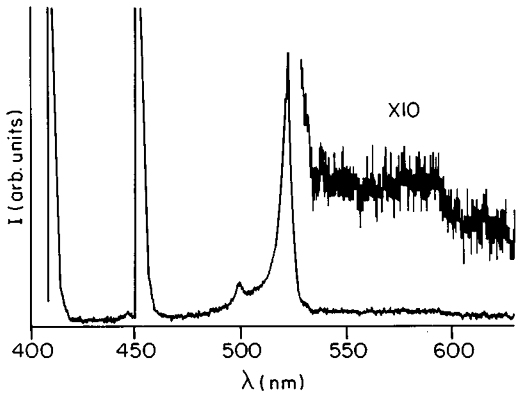

FIG. 1. Visible emission spectra produced when the In($6\,^2S_{1/2}$–$5\,^2P_{1/2}$) transition in an Hg-In vapor at 1173 K is excited at a power density of $0.3\ \mathrm{MW/cm}^2$.

III. RESULTS

Several types of spectroscopic data are reported here. The first is the dispersed emission spectrum following In($6\,^2S_{1/2}-5\,^2P_{1/2}$) excitation at 410.3 nm. The second is dispersed emission following excitation at various points in the 490–525-nm range, which is the region where the HgIn bound-bound emission occurs. A third consists of excitation spectra taken by scanning the laser around the In($6\,^2S_{1/2}$–$5\,^2P_{1/2}$) transition region and over the 490–525-nm region. Finally, measurements were made of the time dependence of the emission decay of some of the spectral transitions following pulsed laser excitation at 410.3 and 522 nm.

Excitation of In($6\,^2S_{1/2}$–$5\,^2P_{1/2}$) at 410.3 nm

The emission spectrum produced when a mercury-indium vapor is excited on the 410.3-nm In($6\,^2S_{1/2}$–$5\,^2P_{1/2}$) resonance transition is shown in Figs. 1–4 with the visible features in Fig. 1 and the UV in Fig. 2. Figure 3 exhibits details of the satellites near the In atomic resonance transitions, and Fig. 4 shows emission details of the HgIn bound-bound transitions at 499 and 522 nm. All intensities are in arbitrary units, and all spectra were obtained at a vapor cell temperature of 1173 K. The features near the In atomic resonance lines that are due to the presence of Hg include the prominent red-wing excimer shoulders at 412.7 and 453.6 nm in Fig. 3 which are identical to those reported for electrical discharge excitation in a Hg-In vapor [8,11]. However, the electrical discharge features previously observed at 455 and 438 nm could not be detected. On the blue side of the 451.1-nm line, the weak satellite observed in an electrical discharge at 447 nm was found in this work, but the satellites

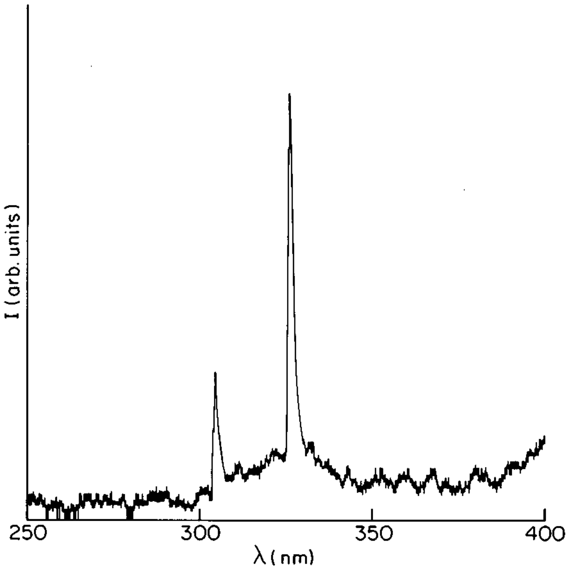

FIG. 2. Ultraviolet emission spectra produced when the In(6 $^2S_{1/2}$–5 $^2P_{1/2}$) transition in an Hg-In vapor at 1173 K is excited at a power density of 3.5 MW/cm^2.

previously reported [11] at 405 and 392 nm are not evident. Other features due to Hg are the HgIn bound-bound transitions at 499 and 522 nm and the Hg enhanced UV emission of the In(5 ^2D–5 $^2P_{1/2,3/2}$) transitions. These latter also exhibit line broadening due to Hg. An additional spectral feature not previously reported is the broad wing on the red side of the transition at 522 nm, which extends to 590 nm. In contrast to measurements made in electrical discharges, the present spectra are free from the complications of self-reversal of the In resonance lines and the presence of Hg atomic transitions.

An excitation spectrum of the Hg-In interaction near the 410.3-nm In resonance line can be obtained by monitoring the 451.1-nm fluorescence as the laser is scanned over the In(6 $^2S_{1/2}$–5 $^2P_{1/2}$) transition as shown in Fig. 5 where it is compared with the very narrow excitation spectrum taken in the absence of mercury. Because of the optical mixing configuration, the available scan range is limited, and the entire width of the In resonance line wings could not be obtained in one excitation scan. With the laser and mixing crystal retuned to 412.7 nm, a scan through this region did not reveal the satellite structure at 412.7 nm in the excitation spectrum.

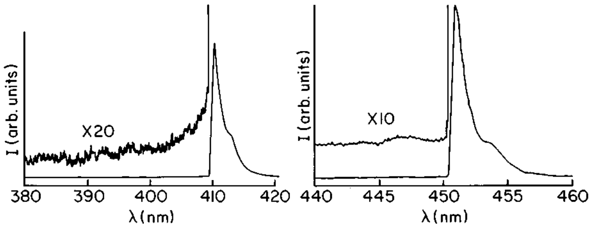

FIG. 3. HgIn excimer emission satellite wings on the In(6 $^2S_{1/2}$–5 $^2P_{1/2}$) and In(6 $^2S_{1/2}$–5 $^2P_{3/2}$) atomic emission lines resulting from excitation of the In(6 $^2S_{1/2}$–5 $^2P_{1/2}$) transition in an Hg-In vapor at 1173 K and at a power density of 1.5 MW/cm^2.

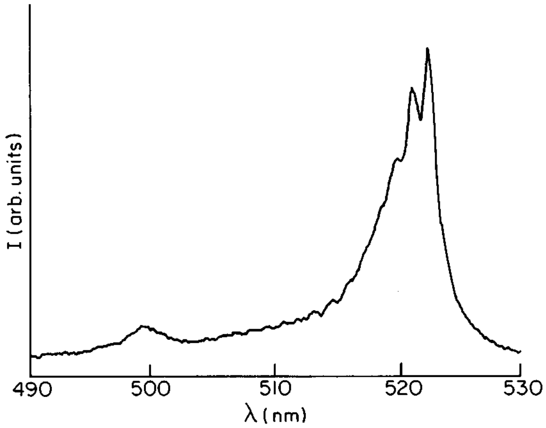

FIG. 4. HgIn bound-bound emission produced in an Hg-In vapor at 1173 K following In(6 $^2S_{1/2}$–5 $^2P_{1/2}$) excitation at a power density of 0.3 MW/cm^2.

The bound-bound HgIn emission bands observed by Purbrick [8] at 499 and 522 nm are also produced by laser excitation of In(6 $^2S_{1/2}$) as shown in Fig. 4. As mentioned above, the 522-nm band was previously observed by Thomson *et al.* in an In(6 $^2S_{1/2}$) excitation experiment where the In atoms were generated by photolysis of InBr in the presence of Hg vapor [10]. In that experiment the 499-nm band was either absent or obscured by a broad, strong emission band at 505 nm, which was reported to be present even in the absence of Hg vapor and was attributed to products of a reaction between excited In(6 $^2S_{1/2}$) and undissociated InBr to form either InBr or In$_2$. The band at 505 nm was not detected in the present work, nor in a previous In(6 $^2S_{1/2}$) excitation study in pure In vapor at higher temperatures to produce emission spectra of In$_2$ [15], ruling out the possibility that the 505-nm band is due to emission by excited In$_2$. In the present work the 522-nm emission was resolved into bands that correspond the (0-0), (1-1), and (2-2) bands found in the high-resolution study of Chilukuri and Winans [9]. The 499-nm band emission observed here as well as in the electric discharge experiment of Purbrick [8], was absent from the HgIn spectra of Chilikuri and Winans. Since the latter authors demonstrated that some of the bands observed

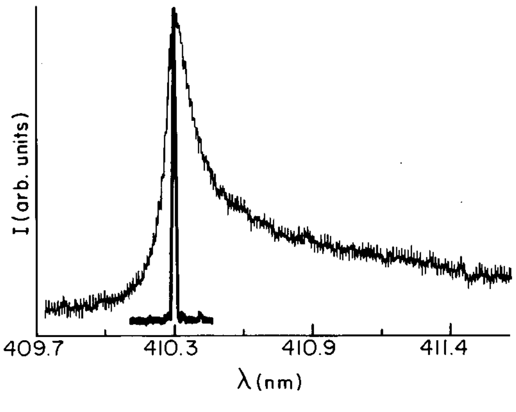

FIG. 5. Excitation spectrum of HgIn taken by scanning 0.8-cm^{-1} linewidth laser radiation at a power density of 1.5 MW/cm^2 across the In(6 $^2S_{1/2}$–5 $^2P_{1/2}$) transition and detecting the In(6 $^2S_{1/2}$–5 $^2P_{3/2}$) emission. For comparison, the narrow In excitation spectrum found under identical conditions but without Hg is shown.

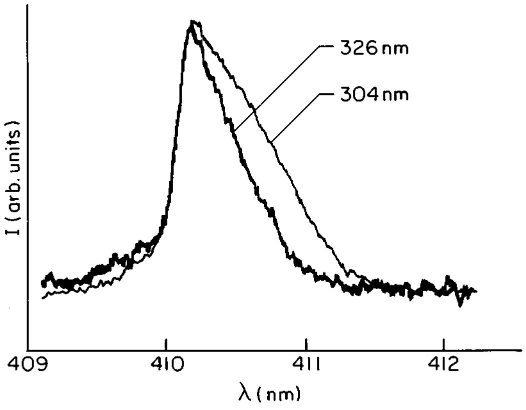

FIG. 6. Excitation spectra of the two In($5\,^2D$) UV atomic emission lines in an Hg-In vapor at 1173 K produced by scanning a laser over the In($6\,^2S_{1/2}$–$5\,^2P_{1/2}$) transition at 410.3 nm at a power density of 3.5 MW/cm^2.

by Purbrick were due to a CdIn impurity, the assignment of 499 nm to HgIn might be called into question, but the observation of the 499-nm band in this work is strong evidence that it is indeed due to HgIn. While the 499-nm band was resolved in the spectra obtained by Purbrick with a 21-ft grating instrument, it is unresolved here. Both the 522- and 499-nm band intensities exhibited linear dependencies on the incident laser power at 410.3 nm and linear dependencies on the In atomic vapor density.

In the present study, a number of emission features were also observed in the UV following the In($6\,^2S_{1/2}$–$5\,^2P_{1/2}$) excitation at 410.3 nm, which would require a multiphoton excitation process. The two principal features shown in Fig. 2 are the In($5\,^2D$–$5\,^2P_{1/2}$) and In($5\,^2D$–$5\,^2P_{3/2}$) atomic transitions at 304 and 326 nm, which can result from either recombination and/or cascade mechanisms involving species that are produced by two-photon excitation. The variation in intensity of these atomic UV features exhibited a linear dependence on laser power at 410.3 nm, but required sufficiently high power levels that the In($6\,^2S_{1/2}$–$5\,^2P_{1/2}$) transition is saturated. For vapor cells that contain only In and Ne at 1173 K, the UV atomic emission at 326 nm is very weak and difficult to observe even with the same laser power levels used here, and the transition at 304 nm is unobservable. The UV emission at 304 nm is never observed in cells with only In and Ne present even at temperatures as high as 1223 K, the highest temperatures used in previous In+Ne experiments [16]. In the present work both of the atomic UV lines are strongly enhanced and broadened when Hg is present. A temperature dependence study of the UV indium atomic line intensities produced by 410.3-nm excitation (carried out at a power of 0.2 MW) reveals that the In atomic UV emission is linear in the indium vapor density. This fact, as well as the linear laser power dependence, rules out an energy pooling mechanism for the production of In($5\,^2D$). Excitation spectra taken by scanning the laser over the In($6\,^2S_{1/2}$–$5\,^2P_{1/2}$) transition and detecting the In($5\,^2D$) emission at 304 and 326 nm are shown in Fig. 6. Their broad widths (which are different for each In transition) are also contrary to an energy pooling process which in In+Ne is known to occur only when the laser excitation is tuned exactly on resonance [16]. Furthermore, the time evolution of the In($5\,^2D$) emission at both 304 and 326 nm exhibits a slightly faster decay rate than the In($6\,^2S_{1/2}$) emission at 451.1 nm and more closely follows the laser pulse. This is consistent with the short (7 ns) lifetime of In($5\,^2D$). The production of 326-nm emission by In($6\,^2S_{1/2}$)+In($6\,^2S_{1/2}$) energy pooling ionization collisions occurs with a time delay due to In$^+ + e^-$ recombination and energy cascade to In($5\,^2D$) [16]. No such delay is observed here, which is not only further evidence against an energy pooling process, but also argues against a multiphoton ionization (MPI) route to In($5\,^2D$). The broad widths observed here indicate that a multiphoton excitation route to eventual formation of the In($5\,^2D$) excited states involves the Hg-In colliding pair. A linear power dependence of the atomic UV emission intensity results if the In($6\,^2S_{1/2}$) excitation is saturated, which is the case here. Since there are a number of mercury dimer electronic states in the same energy range as In($5\,^2D$) and since the mercury density is approximately 10^{19} cm^{-3}, it is reasonable to expect population of these states via collisional energy transfer from any excited HgIn states which generate In($5\,^2D$). While weak features appear near the 304- and 326-nm In atomic lines in the UV, these are as yet unidentified. However, it should be pointed out that the broad feature near the base of the 326-nm In line may be due to emission from the Hg$_2$(1_u) state that correlates with Hg($6\,^3P_1$), the emission of which peaks at 335 nm [17].

In order to further characterize the nature of the electronic states associated with the HgIn bound-bound transitions at 499 and 522 nm, additional fluorescence decay measurements were obtained. Figure 7 shows the time dependence of the fluorescence decay at 522-nm following In($6\,^2S_{1/2}$–$5\,^2P_{1/2}$) pulsed excitation, which exhibits both a fast and a slow component. The branching ratio between the fast and slow components as a function of temperature is shown in Fig. 7, with the slow component dominating the decay at 1173 K. Under conditions of saturation of the $6\,^2S_{1/2}$ state of In, the branching ratios are not functions of laser power. The fast component has a time constant identical to the 25±2 ns decay of the In($6\,^2S_{1/2}$) state [18], while that of the slow component is 106±11 ns. The time decay of the In($6\,^2S_{1/2}$–$5\,^2P_{3/2}$) emission at 451.1 nm resulting from In($6\,^2S_{1/2}$–$5\,^2P_{1/2}$) excitation similarly exhibits a slow tail with a 92±18 ns time constant. Both the 522-nm emission and the In($6\,^2S_{1/2}$) emission have, therefore, roughly the same decay kinetics under these conditions. Since there is both a fast and a slow component to each of these emission features, it is likely that two interactions or decay pathways are making a contribution. The fast component at 522 nm is consistent with the correlation of the 522-nm radiating state with In($6\,^2S_{1/2}$)+Hg($6\,^1S_0$) since In($6\,^2S_{1/2}$) also has a fast decay of 25±2 ns and its transition moment for emission would dominate the transition dipole of the correlated HgIn state. The slow component could arise from cascade into In($6\,^2S_{1/2}$) from some long-lived reservoir states at higher energy. There are many HgIn possibilities for such states, and one must include those that correlate with the long-lived triplet states of Hg: $6\,^3P_0$, $6\,^3P_1$, $6\,^3P_2$, which are the only excited Hg-atom states that lie below the ionization energy of the In atom. There is also a possibility that the responsible reservoir states may be derived from Hg$_2$.

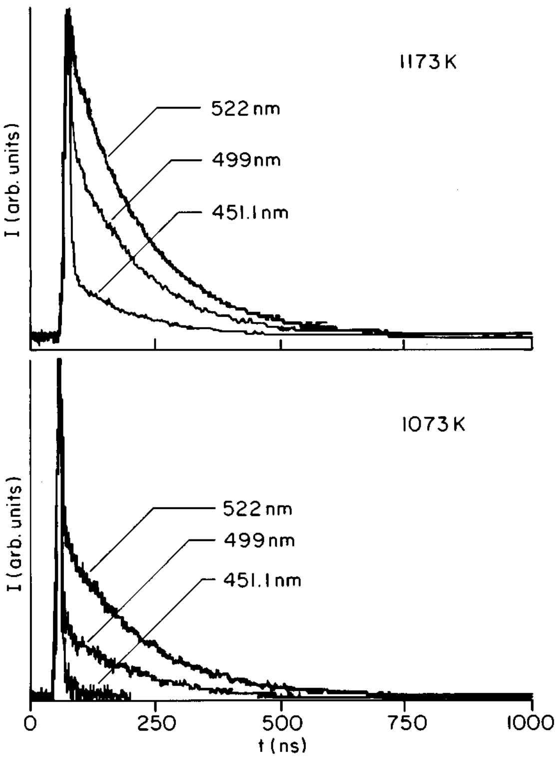

FIG. 7. The time evolution of the 522- and 499-nm band HgIn emission and the 451.1-nm In(6 $^2S_{1/2}$–5 $^2P_{3/2}$) atomic emission at different temperatures in the Hg-In vapor following pulsed excitation of the 410.3-nm In(6 $^2S_{1/2}$–5 $^2P_{1/2}$) transition at a power density of 1.5 MW/cm^2.

Direct excitation of HgIn at 522 nm

Direct excitation of the HgIn bound-bound transition at 522 nm produces weak indications of unresolved structure around the scattered laser radiation. However, strong fluorescence at 410.3 and 451.1 nm is also produced, exhibiting a linear dependance on laser excitation power at 522 nm. Using the detection of emission at either of the In atomic resonance wavelengths, an excitation spectrum of HgIn can be obtained by scanning the exciting laser through the 522-nm region as shown in Fig. 8. The observed band structure closely corresponds to the emission spectra resulting from In(6 $^2S_{1/2}$) excitation and to the known high-resolution emission spectrum [8,9] with the (0-0), (1-1), and (2-2) vibrational bands again evident. Direct excitation at 499 nm produces only very weak emission at 410.3 and 451.1 nm as well as some fluorescence near 499 nm, but no emission at any other wavelengths between 525 and 300 nm. None of the UV features that appear when the In(6 $^2S_{1/2}$) state is excited on one of the In resonance transitions are produced as a result of excitation in the 490–525-nm region.

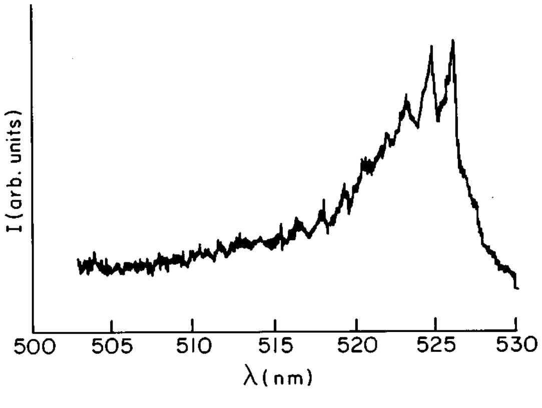

FIG. 8. Laser excitation spectrum of the 522-nm band produced by scanning 0.3-cm^{-1} linewidth laser radiation at a power density of 0.7 MW/cm^2 across the band and detected as emission on the In(6 $^2S_{1/2}$–5 $^2P_{1/2}$) atomic transition.

The rate of emission at the In atomic resonance frequencies following 522-nm pulsed excitation also exhibits fast and slow decay components. The fast component is again consistent with the 25±2 ns In(6 $^2S_{1/2}$) decay [18], and the slow components are 132±13 ns for the In(6 $^2S_{1/2}$–5 $^2P_{3/2}$) emission, and 106±8 ns for the In(6 $^2S_{1/2}$–5 $^2P_{1/2}$) emission. The fluorescence lifetime of the 522-nm emission under the same excitation conditions exhibits the same fast component plus a much longer tail with a time constant of 250±75 ns. As above, the slow components of the In atomic resonance transitions are consistent with the production of long-lived reservoir states, which cascade into In(6 $^2S_{1/2}$). These may be the same as those that are accessed using the In(6 $^2S_{1/2}$) state excitation at 410.3 nm since the time constants for the slow emission components are similar. However, an additional, longer-lived reservoir state participates in the cascade to the 522 nm emitting state when the excitation is induced at 522 nm.

IV. DISCUSSION

In order to accommodate the previous spectroscopic findings together with the present observations, a proposed set of potential-energy curves is schematically presented in Fig. 9.

As discussed by Pichler *et al.* [11] some guidance for the construction of a HgIn potential-energy diagram can be obtained from both theoretical [12] and experimental [19,20] studies of HgTl. Experiment shows that the corresponding $B\ ^2\Sigma_{1/2}$ and $X_{3/2}$ states of HgTl have binding energies of about 4400–4600 and 1240–2750 cm^{-1}, respectively. The binding energy of the HgTl($X_{1/2}$) ground state appears to be 800 cm^{-1}. The HgTl($B\ ^2\Sigma_{1/2}$) excited state is also predicted [12] to have a large contribution from a strongly attractive ion-pair configuration which makes an avoided crossing with the repulsive potential arising from Tl(7 $^2S_{1/2}$)+Hg(6 $^1S_0$). Pichler *et al.* made an analogy between the electronic states of HgIn and those of HgTl to explain the satellite band structure around the In atomic resonance lines in an HgIn electrical discharge. In order to reconcile the present spectroscopic findings with the previous assignments of HgIn spectra and the extrapolation from HgTl, several new features are required and are incorporated into the schematically drawn potential-energy curves of Fig. 9. Most prominent of these are the deep wells associated with the $B\ ^2\Sigma_{1/2}$ and $X_{3/2,1/2}$ states, which are projected to be the upper and lower electronic states responsible for the bound-bound transition at 522 nm.

Because the 522-nm band can be produced by In(6 $^2S_{1/2}$) excitation, Thomson *et al.* assigned it to emission arising from the bound excimer state of HgIn correlating with the In(6 $^2S_{1/2}$)+Hg(6 $^1S_0$) asymptote. They also suggested [10]

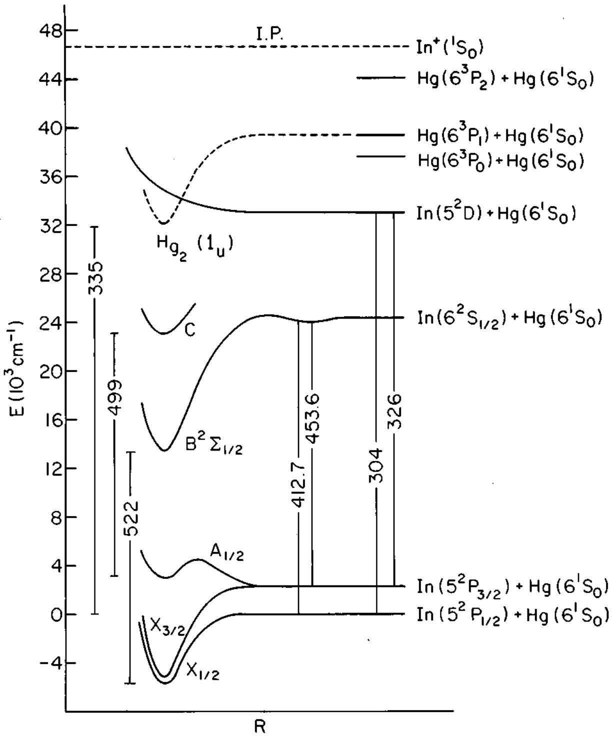

FIG. 9. Schematically drawn potential-energy diagram for HgIn incorporating features which are necessary for consistency with the spectroscopic observations observed previously and in the present work. Also shown is the energetic location of the $\mathrm{Hg}_2(1_u)$ state (dashed curve), which can participate in energy transfer collision with excited HgIn or In and which can emit 335-nm radiation in its transition to the unbound ground state (not shown) of Hg_2 located at $E=0$.

that the lower state correlated with $\mathrm{In}(5\,^2P_{3/2})+\mathrm{Hg}(6\,^1S_0)$. As pointed out above, the spectral analysis of Chilukuri and Winans [9] implies that both the upper and lower states for the 522-nm band are deeply bound. In fact, if the potential-energy curves could be modeled by Morse potentials, approximate values for the dissociation energies can be found from $D_e=\omega_e^2/4\omega_e x_e$. Using the ω_e values from Chilukuri and Winans and the assumption that $\omega_e x_e$ is less than $0.5\ \mathrm{cm}^{-1}$ for HgIn (Chilukuri and Winans set $\omega_e x_e \approx 0$), dissociation energies in excess of $10^4\ \mathrm{cm}^{-1}$ would be required by a Morse potential for the upper and lower states which produce the 522-nm band. This fact plus the $22\,159\text{-cm}^{-1}$ difference between the $\mathrm{In}(6\,^2S_{1/2})+\mathrm{Hg}(^1S_0)$ and $\mathrm{In}(5\,^2P_{1/2})+\mathrm{Hg}(^1S_0)$ asymptotes, the 2212.58-cm^{-1} $\mathrm{In}(5\,^2P_{3/2}-5\,^2P_{1/2})$ fine-structure separation, together with the measured 522-band origin [8,9] of $\nu_e=19\,106\ \mathrm{cm}^{-1}$ requires substantial binding for the upper and lower electronic states of the 522-nm transition. If the lower state of the 522-nm band were correlated only with $\mathrm{In}(5\,^2P_{3/2})$, an unbound, repulsive HgIn ground state correlating with $\mathrm{In}(5\,^2P_{1/2})+\mathrm{Hg}(6\,^1S_0)$ would not be possible. Even if the HgIn electronic states depart significantly from a Morse model, the negligible $\omega_e x_e$ values must indicate deeply bound states. This can be accommodated by the $X_{3/2,1/2}$ HgIn states schematically sketched in Fig. 9, both being deeply bound.

In the reinterpretation of Purbrick's spectra [8] by Chilikuri and Winans [9] the 522 band contained a $^2\Pi$ fine-structure separation that was very small compared to the similar separation of $20\ \mathrm{cm}^{-1}$ in ZnIn and $8\ \mathrm{cm}^{-1}$ in CdIn, which they point out indicates an approach of the $^2\Pi$ state to Hund's case (b) in the trend from lighter to heavier molecules. However, Chilikuri and Winans also placed the $^2\Pi$ state above the $^2\Sigma$ on the basis of relative intensities of the P and R branches, which is the reverse of the requirement here that the lower state is $^2\Pi$. In the present work the upper state of the 522-nm band is generated by a one-photon excitation of $\mathrm{In}(6\,^2S_{1/2})$, and the 522-nm emission has a fast component identical to the decay rate of $\mathrm{In}(6\,^2S_{1/2})$, which is further evidence that the upper state for the 522-nm band correlates with $\mathrm{Hg}(6\,^1S_0)+\mathrm{In}(6\,^2S_{1/2})$, in agreement with Thomson *et al.*, and therefore must be a $^2\Sigma_{1/2}$ state. Furthermore, the fact that the 522-nm emission can be directly excited with a one-photon process requires that the lower state must correlate with one (or both) $\mathrm{In}(^2P)$ ground states. The long-time components of the decay rates arise from multiphoton excitation processes that decay by cascade through longer-lived higher excited states of HgIn or Hg_2.

Figure 9 for HgIn departs from an extrapolation of the theoretical curves for HgTl in that the ground-state fine structure components are close together and are more deeply bound. This is reasonable since the $6\,^2P_{3/2}-6\,^2P_{1/2}$ fine-structure interval is much larger in Tl than the $5\,^2P_{3/2}-5\,^2P_{1/2}$ separation in In: $7792.7\ \mathrm{cm}^{-1}$ for Tl compared to $2212.58\ \mathrm{cm}^{-1}$ for In. In Fig. 9, the ground state has been designated $X_{3/2,1/2}$ corresponding to the notation for HgTl used by Pfaff and Stock [19] and Chilikuri and Winans [20]. It is suggested that the 522-nm band in HgIn should be referred to as the B-X transition rather than B-A as used by Purbrick [8] and Chilikuri and Winans [9].

The weaker transition at 499 nm was shown to have resolved structure by Purbrick [8], but with vibrational band separations in the $40–50\text{-cm}^{-1}$ range, quite different from that of the 522-nm band. In the present work, the 499-nm band is produced in emission by excitation of In to the $6\,^2S_{1/2}$ state but is unresolved. Direct excitation at 499 nm produces $\mathrm{In}(6\,^2S_{1/2})$ but with greatly diminished intensity when compared to excitation at 522 nm. Furthermore, excitation at 499 nm does not produce measureable emission at 522 nm. A consistent explanation for these facts is the $C\,^2\Sigma_{1/2}$–$A\,^2\Sigma_{1/2}$ assignment for 499-nm shown in Fig. 9. The upper and lower bound states for this transition are not required to be as deep as those for the 522-nm transition. While the upper state for the 499-nm band is not the same as that which gives rise to the 522-nm emission, it is nevertheless diabatically correlated with $\mathrm{In}(6\,^2S_{1/2})+\mathrm{Hg}(6\,^1S_0)$. The lower $A\,^2\Sigma_{1/2}$ state lies above the $X_{3/2,1/2}$ states and is weakly thermally accessible. The upper $C\,^2\Sigma_{1/2}$ state can be populated from $\mathrm{In}(6\,^2S_{1/2})$ by diabatic collisions with $\mathrm{Hg}(6\,^1S_0)$. The broad diffuse emission that extends from the 522-nm transition to 590 nm may be bound-free emission from either the $C\,^2\Sigma^2_{1/2}$ or $B\,^2\Sigma_{1/2}$ states to the $A\,^2\Sigma_{1/2}$ or $X_{3/2,1/2}$ states. Finally, the red-wing satellites on the In atomic resonance lines are given, in agreement with Pichler *et al.*, to regions where the $\mathrm{In}(6\,^2S_{1/2}-5\,^2P_{3/2})$ and $\mathrm{In}(6\,^2S_{1/2}-^2P_{1/2})$ difference potentials are less than the resonant state separations and remain constant over a region of Hg-In internuclear distances.

A complete analysis of the radiative and nonradiative decay kinetics of the excited states would require a detailed investigation of the fluorescence lifetimes as a function of the densities and collision rates among all species present. While such an energy transfer study was beyond the scope of the present survey, the fluorescence decay lifetimes measured here support the proposed assignments in Fig. 9. The present spectroscopic findings are consistent with the 522-nm transition being dominated by the strong In($6\,{}^2S_{1/2}$–$5\,{}^2P_{3/2,1/2}$) transition moments.

V. SUMMARY

While the satellite structure on the In atomic resonance transitions may very well have excimer emission characteristics, the HgIn bound-bound transition appears to indicate substantially binding for the ground electronic state of HgIn, which is not conducive to high gain for HgIn excimer emission in general.

This conclusion is consistent with the spectroscopic interpretations that (a) give negligible anharmonic constants for the upper and lower electronic states responsible for the 522-nm bound-bound transition; (b) require the upper electronic state of the 522-nm transition to be correlated with In($6\,{}^2S_{1/2}$)+Hg($6\,{}^1S_0$); (c) assign the 522-nm transition to a ${}^2\Sigma_{1/2}$–$X_{3/2,1/2}$ transition with a small X-state fine-structure separation; and (d) reveal a transition probability for the 522-nm emission that is identical to the In($6\,{}^2S_{1/2}$) emission. Other results include a probable assignment of the weak 499-nm band and the possible existence of several longer-lived HgIn and/or Hg_2 reservoir states that lie above the HgIn $B\,{}^2\Sigma_{1/2}$ state that participate in the decay following resonant multiphoton excitation via the In($6\,{}^2S_{1/2}$) atomic state or the HgIn $B\,{}^2\Sigma_{1/2}$ state. Full characterization of the $X_{3/2,1/2}$ states of HgIn would benefit from studies conducted on HgIn cooled in supersonic beam expansions.

ACKNOWLEDGMENTS

Support from the National Science Foundation, NATO, and the Italian Consiglio Nazionale della Ricerche is gratefully acknowledged.

[1] A. Gallagher in *Excimer Lasers*, edited by Ch. K. Rhodes (Springer-Verlag, Berlin, 1984), p. 139.

[2] J. H. Parks, Appl. Phys. Lett. **31**, 192 (1977).

[3] S. Chilukuri and M. H. Nayfeh, J. Appl. Phys. **49**, 5378 (1978).

[4] C. E. Moore, *Atomic Energy Levels*, NBS Circular No. 467 (U.S. Government Printing Office, 1958), Vol. III, pp. 64–66.

[5] P. Bicchi, A. Kopystynska, M. Meucci, and L. Moi, Phys. Rev. A **41**, 5257 (1990).

[6] P. Bicchi, C. Marinelli, E. Mariotti, M. Meucci, and L. Moi, J. Phys. B **30**, 473 (1997).

[7] J. G. Winans, F. J. Davis, and V. A. Leitzke, Phys. Rev. **57**, 70 (1940).

[8] R. L. Purbrick, Phys. Rev. **81**, 89 (1951).

[9] S. Chilukuri and J. G. Winans, J. Mol. Spectrosc. **16**, 309 (1965).

[10] R. G. C. Thomson, I. Duncan, and T. Morrow, Chem. Phys. Lett. **187**, 396 (1991).

[11] G. Pichler, D. Azinovic, and R. Beuc, Fiz. A **2**, 1 (1993).

[12] K. C. Celestino and W. C. Ermler, J. Chem. Phys. **81**, 1872 (1984).

[13] The In sample was obtained from the Fluka Company.

[14] A. N. Nesmeyanov, *Vapor Pressure of the Chemical Elements*, (Elsevier, Amsterdam, 1963), p. 447.

[15] P. Bicchi, C. Marinelli, and R. A. Bernheim, J. Chem. Phys. **97**, 8809 (1992).

[16] P. Bicchi, C. Marinelli, E. Mariotti, M. Meucci, and L. Moi, J. Phys. B **26**, 2335 (1993).

[17] R. E. Drullinger, M. M. Hessel, and E. W. Smith, J. Chem. Phys. **66**, 5656 (1977).

[18] P. Bicchi, C. Marinelli, E. Mariotti, M. Meucci, and L. Moi, Opt. Commun. **106**, 197 (1994).

[19] J. Pfaff and M. Stock, J. Chem. Phys. **77**, 2928 (1982).

[20] S. Chilukuri, W. J. Pearce, and J. G. Winans, J. Chem. Phys. **82**, 4405 (1985).